Particle & Particle Systems Characterization
www.particle-journal.com

Sonofragmentation of Ultrathin 1D Nanomaterials

*Ruixuan Gao, Ishan Gupta, and Edward S. Boyden**

Small (<10 nm) nanoparticles (NPs) are important because of the unique physical and chemical properties that arise due to their small size and large surface area.[1–9] A multitude of methods have been developed to produce such NPs.[10] Top-down synthesis methods that rely on breaking down bulk materials into smaller fragments can be scalably deployed.[11–21] However, the method struggles with monodispersity and with percent yield for such small NPs. Bottom-up synthesis methods can effectively assemble small molecule precursors into larger units to create small NPs.[22–35] However, both methods require harsh chemicals[20,34] or specialized equipment,[13,21,27,29,35] out of reach from many end users. Ideally, one could obtain extremely monodisperse NPs of small size and high yield on regular benchtop equipment on site.

We here propose a top-down method of NP synthesis that results in high-monodispersity NPs. We hypothesized that nanowires of extreme aspect ratio could be ultrasonicated to generate NPs. This hypothesis builds from recent studies[36–40] that show ultrasonication can be used to break down nanowires into shorter nanowires, and nanotubes into shorter nanotubes. We hypothesized that by choosing nanowires of high aspect ratio, and then applying ultrasonication, it would be possible to perform top-down synthesis of many kinds of NPs in effectively a single step. We note that the final yield of the NP synthesis would depend on the yield and supply of the starting materials, some of which require specialized equipment and precursors. With a constant supply of the nanowires, our method would enable scalable production of ultrasmall NP production in large quantities. Such nanowire production could be realized by, for example, a catalyzed high-throughput gas phase synthesis with extremely high precursor efficiency and gram-scale yield.[41]

We set out to test our hypothesis using ultrathin Ge nanowires (**Figure 1**a). Up to date, synthesis of Ge NPs (<10 nm) has been limited to gas-phase and liquid phase approaches that require expensive machines,[42] and top-down approaches that do not yield monodisperse crystalline NPs.[12,43] Therefore, a simple and inexpensive method for top-down synthesis of Ge NPs would be potentially of both scientific and commercial interest.

Dr. R. Gao, I. Gupta, Prof. E. S. Boyden
Media Lab
Massachusetts Institute of Technology
Cambridge, MA 02139, USA
E-mail: esb@media.mit.edu
I. Gupta, Prof. E. S. Boyden
Department of Biological Engineering
Massachusetts Institute of Technology
Cambridge, MA 02139, USA
Prof. E. S. Boyden
McGovern Institute for Brain Research
Massachusetts Institute of Technology
Cambridge, MA 02139, USA

DOI: 10.1002/ppsc.201600339

We first dispersed ultrathin Ge nanowires[44] (diameters tapering from ≈30 nm to ≈2 nm) in dimethylformamide (DMF), and ultrasonicated the suspension with a bench-top ultrasonicator (40 kHz, 110 W). To track fragmentation of the nanowires, we imaged the ultrasonicated sample at different time points using scanning electron microscopy (SEM) (Figure 1b top row, Figure S1, Supporting Information). We found that the nanowires readily fragmented into <30 nm particles within 30 minutes of ultrasonication. The particle size further decreased with increasing ultrasonication time. For instance, the majority of the NPs had diameters of <10 nm with 18 h ultrasonication. As comparison, we carried out the same ultrasonication using a non-1D Ge substrate (100–300 nm diameter nanopowder) (Figure 1b bottom row, Figure S2, Supporting Information). In contrast to the nanowires, the nanopowder did not show a clear change in particle size with increasing ultrasonication time. For instance, after 18 h of ultrasonication, we observed mostly ≈100–300 nm particles, comparable to the size distribution of the starting material.

We analyzed Ge NPs produced after 18 h of nanowire ultrasonication using transmission electron microscopy (TEM). NPs were resuspended in ethanol, filtered through a 0.2 µm filter to remove large debris and aggregates, and drop-casted and dried on a copper/carbon grid (**Figure 2**a). Analysis of bright-field TEM images shows the NPs had an average size of 3.58 nm and a standard deviation of 0.74 nm ($n = 75$ from a single TEM grid; Figure 2b), confirming generation of ultrasmall (<10 nm) Ge NPs. Furthermore, high-resolution TEM (HRTEM) imaging of a typical Ge NP showed clear lattice fringes, indicating minimal amorphization effect during the long-term ultrasonication (Figure 2a, inset). The ≈0.20 nm spacing of lattice fringes corresponds to the spacing between (220) planes of Ge, consistent with the starting material, crystalline Ge nanowires.[45] In addition to 18 h ultrasonicated NPs, we imaged Ge NPs after 30 min and 1 h of ultrasonication with TEM (Figure S3, Supporting Information). The results show a size change consistent with the previous SEM experiments.

We further carried out dynamic laser scattering (DLS) analysis of the ultrasonicated Ge nanowire product. Consistent with the TEM analysis, we found that monodisperse (polydispersity (Pd) = 6.8%) Ge NPs of 2–5 nm diameter were generated after 18 h of ultrasonication, with no further purification (Figure 2c). We also carried out a temperature-controlled sonofragmentation experiments with two different temperature ranges of 10–20 °C and 60–65 °C (Figure S4, Supporting Information). The results show that within the range of temperatures encountered throughout such sonication experiments, the precise temperature value had minimal effect on the synthesized NP size distribution. In comparison to the Ge nanowire substrate, the Ge nanopowder substrate showed similar NP size range and distribution before (Pd = 16.2%) versus after an ultrasonication time of 36 h (Pd = 19.1%) (Figure S5, Supporting Information).

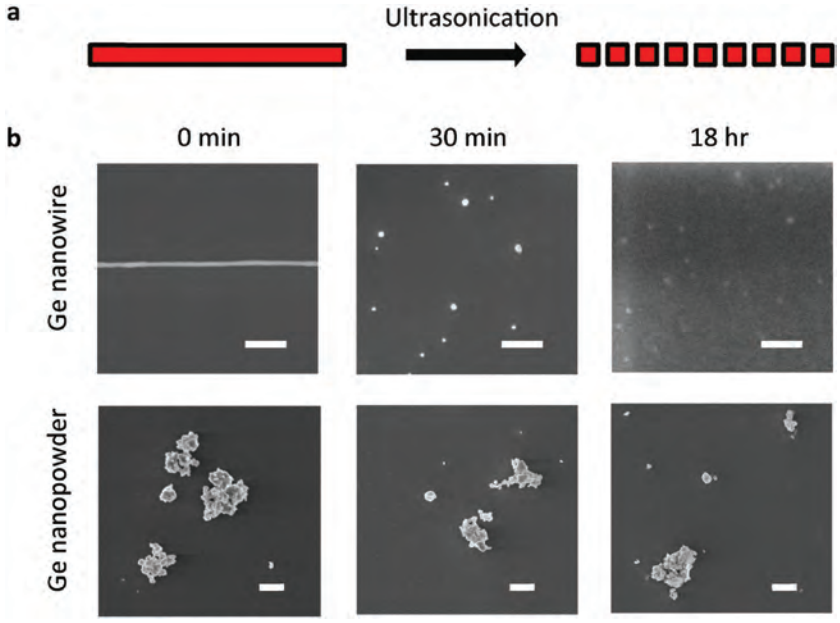

Figure 1. Synthesis of <10 nm nanoparticles (NPs) via sonofragmentation. a) Schematic of sonofragmentation of a high-aspect-ratio 1D nanostructure into NPs. b) Top row: scanning electron microscopey(SEM) images of an ultrathin Ge nanowire (left) and fragments after 30 min (center) and 18 h (right) of ultrasonication. Scale bars, 200 nm. Bottom row: SEM images of Ge nanopowder before (left) and after 30 min (center) and 18 h (right) of ultrasonication. Scale bars, 1 μm.

This result further suggests the advantage of using an ultrathin 1D substrate to produce monodisperse ultrasmall NPs.

To investigate optical properties of the synthesized Ge NPs, we measured the absorbance of the ultrasonicated sample using a UV–vis spectrometer (Figure 2d, blue). We found the Ge NPs readily absorbed light with <400 nm wavelength.[46] Next, we measured the intrinsic photoluminescence (PL) of the Ge NPs under optical excitation using a fluorescence spectrometer. The sample showed a characteristic PL peak around 410 nm wavelengths, consistent with previous reports (Figure 2d, red).[24] We note that the blue emission observed may arise from surface oxidation and absorption of molecules.[24]

To study the surface of the synthesized Ge NPs, we performed Fourier transform infrared (FTIR) spectroscopy on the NPs (Figure 2e). The ultrasonicated Ge NPs were washed in chloroform three times and re-suspended in chloroform. The suspension was then drop-casted and air dried on the attenuated total reflection (ATR) crystal for the FTIR measurements. The surface of the as-synthesized Ge NPs displayed both free hydroxyls (3334 cm^{-1}) and DMF, which may have been chemisorbed onto the surface through a C–O–Ge (1668 cm^{-1}) bridge.[47] We further studied the surface of the NPs after solvent exchanges and found that the DMF molecules were retained after exchanges to ethanol and water.

To assess whether our method can be applied to different types of 1D substrates, we explored synthesis of NPs using various commercially available nanowires, including oxide and metal nanowires. We first carried out ultrasonication of commercially available TiO_2 nanowires (≈10 nm diameter, **Figure 3**a) in water for 24 h. TEM analysis shows that the average and standard deviation of the NP size were 4.63 nm and 1.28 nm, respectively, confirming generation of NPs of <10 nm diameter (Figure 3b,c). HRTEM image of a typical TiO_2 NP showed clear lattice fringes, indicating that the NPs were crystalline (Figure 3b, inset). The ≈0.28 nm spacing between fringes was consistent with the spacing between (100) planes of rutile TiO_2.[48] We also characterized the TiO_2 NPs in the solvent and found the NPs has a monodisperse size distribution (Pd = 11%) of ≈3–6 nm diameter, a range consistent with the TEM analysis (Figure 3d).

Next we carried out ultrasonication of commercially available Ag nanowires (≈20 nm diameter, Figure 3e) using the same sonofragmentation process as the TiO_2 nanowires. TEM characterization shows the synthesized Ag NPs were crystalline and had average size and size standard deviation of 3.46 nm and 0.75 nm, respectively (Figure 3f,g). The HRTEM image of a typical Ag NP showed a lattice fringe spacing of ≈0.24 nm, consistent with the (111) plane spacing of Ag (Figure 3f, inset).[49] We also measured the NP size in the solvent and the results showed a monodisperse size distribution (Pd = 15%) of ≈2–7 nm diameter, consistent with the TEM results (Figure 3h).

Finally, we carried out ultrasonication of Si nanowires[50,51] (≈30 nm diameter, Figure 3i) in DMF for 24 h. TEM analysis shows that the Si NPs were crystalline and the average and standard deviation of the NP size were 10.8 and 2.2 nm, respectively (Figure 3j,k). HRTEM image of a typical Si NP showed a ≈0.27 nm spacing between the lattice fringes, which likely corresponds to the spacing between (200) planes of the diamond cubic lattice of Si (Figure 3j, inset).[52] We note that in this particular image, the commonly observable (111) fringes were not clearly resolved. To characterize the NP size in the solvent, we measured the NP size using DLS. The results show a monodisperse size distribution (Pd = 11.5%) of ≈10–12 nm diameter, a range consistent with the TEM results (Figure 3l). Furthermore, to characterize optical properties of the synthesized Si NPs, we measured the PL of suspension. The results show a violet-blue fluorescence peak at around 400 nm in wavelength, consistent with previous reports (Figure S6, Supporting Information).[53,54]

Based on previous theoretical and experimental studies of ultrasonication,[36–40,55–57] we think the effects of long-term and continuous sonofragmentation on ultrathin nanowires are two-fold: physical and chemical. In a previous study that used a theoretical model to calculate the tensile stress applied by a cavitation bubble, such stress on a 1D nanostructure is shown to be dependent on the ratio of its diameter to its length.[33] The model suggests that thinner and longer nanowire and nanotube substrates can be more easily broken into fragments compared with substrates of low aspect ratio.[36] In another mechanical study, it had been predicted and shown for the case of carbon nanotubes that shorter nanofragments are produced with increasing sonication times.[37] Our observation of NP generation from ultrasonication of high-aspect-ratio nanowires

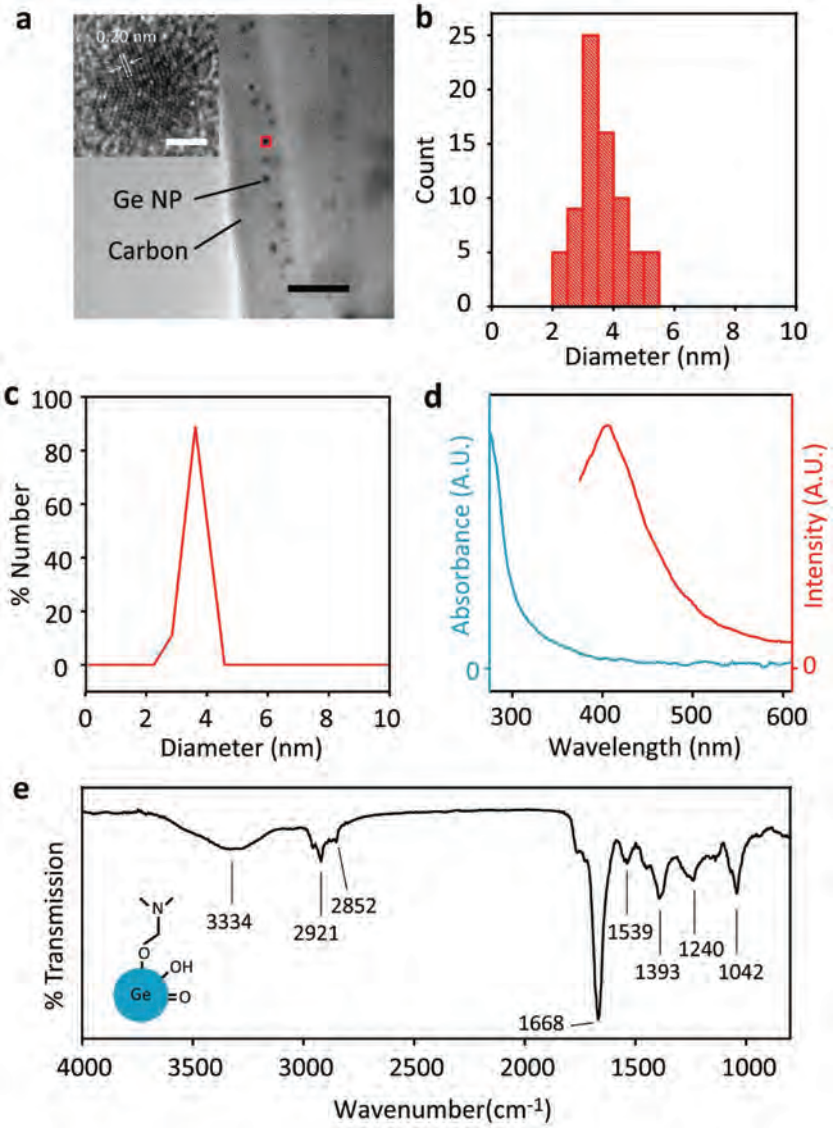

Figure 2. Sonofragmented Ge NPs. a) Transmission electron microscopey(TEM) image of sonofragmented Ge NPs after 18 h ultrasonication of Ge nanowires in dimethylformamide (DMF). Scale bar, 50 nm. Inset, high-resolution TEM (HRTEM) image of a single Ge NP (red box). Scale bar, 2 nm. b) Size distribution of the Ge NPs measured with TEM. The mean (μ) and standard deviation (σ) of the NP size, and the number of NPs analyzed (n) were 3.58 nm, 0.74 nm, and 75, respectively. c) Size distribution of the Ge NPs measured with dynamic laser scattering (DLS) after 18 h ultrasonication of Ge nanowires in DMF. d) UV–vis absorbance spectrum of the Ge NPs in DMF after 18 h ultrasonication (blue) and photoluminescence (PL) of the Ge NPs in ethanol under 320 nm UV-illumination (red). For the PL measurement, the ultrasonication was carried out in DMF for 24 h and the Ge NPs were resuspended in ethanol. e) Fourier transform infrared (FTIR) spectra of Ge NPs ultrasonicated in DMF for 24 h and resuspended in chloroform. Inset, schematic of possible functional groups on the Ge NP surface.

is consistent with these predictions and observations. Aside from mechanical fragmentation of nanowires, significant local heating up to a few thousand Kelvin near the cavitation bubbles could potentially be another cause of nanowire fragmentation.[58] Previous studies have shown that metal and semiconductor nanowires, driven by the Plateau–Rayleigh instability, readily form a string of nanospheres when heated.[59,60] The thermal instability of ultrathin nanowires could in principle be another physical route for NP generation during ultrasonication.

From a chemical point of view, surface functionalization of the NPs plays an important role in dispersing and stabilizing NPs in solvents during sonofragmentation.[61,62] For instance, the FTIR analysis of ultrasonicated Ge NPs suggests that the NP surface is terminated with DMF molecules with CO groups coordinating to Ge atoms. We suspect that these surface coordinated solvent molecules stabilize NPs and prevent them from fast oxidation and decomposition. In addition, the positive charge on the nitrogen terminal may prevent the Ge NPs from aggregating in polar solvents such as DMF and ethanol and thus keep the NPs dispersed in these solvents.

Our time-evolution experiment of the Ge fragments provides further insight into possible mechanisms of NP generation during sonofragmentation. During the initial phase of ultrasonication, Ge nanowires rapidly fragment into <30 nm particles. This process is complete within ≈30 min, which is likely due to the high aspect ratio of the nanowire substrate. Increasing ultrasonication time further reduces the size of these particles: with 18 h of ultrasonication, the NP size range decreased to 3–5 nm.

Future investigation awaits on both theoretical and experimental fronts. Additional theoretical modeling for sonofragmentation of ultrathin inorganic substrates of different materials, diameters and lengths as well as mechanical properties might be explored. In addition, it may be of interest to test specific substrate-solvent combinations and observe the effect of different solvents and surfactants on different substrates and on the sonofragmentation process itself. Furthermore, post-sonofragmentation surface modifications could further tune and improve physical and chemical properties of the synthesized NPs.

In this report, we presented a new method of NP synthesis based on sonofragmentation of ultrathin 1D substrates. We discovered that short-term ultrasonication of high-aspect-ratio 1D substrates could rapidly generate highly monodisperse NPs, and that subsequent longer-term ultrasonication could result in ultrasmall NPs. We believe our method opens up a new approach, which is implementable with a bench-top ultrasonicator, to synthesize NPs of high purity, crystallinity and monodispersity. Thus, our methodology may help democratize small NP production, potentially opening up doors in a variety of fields that would benefit from the use of small NPs for their chemical and physical properties.

Particle
& Particle Systems Characterization
www.particle-journal.com

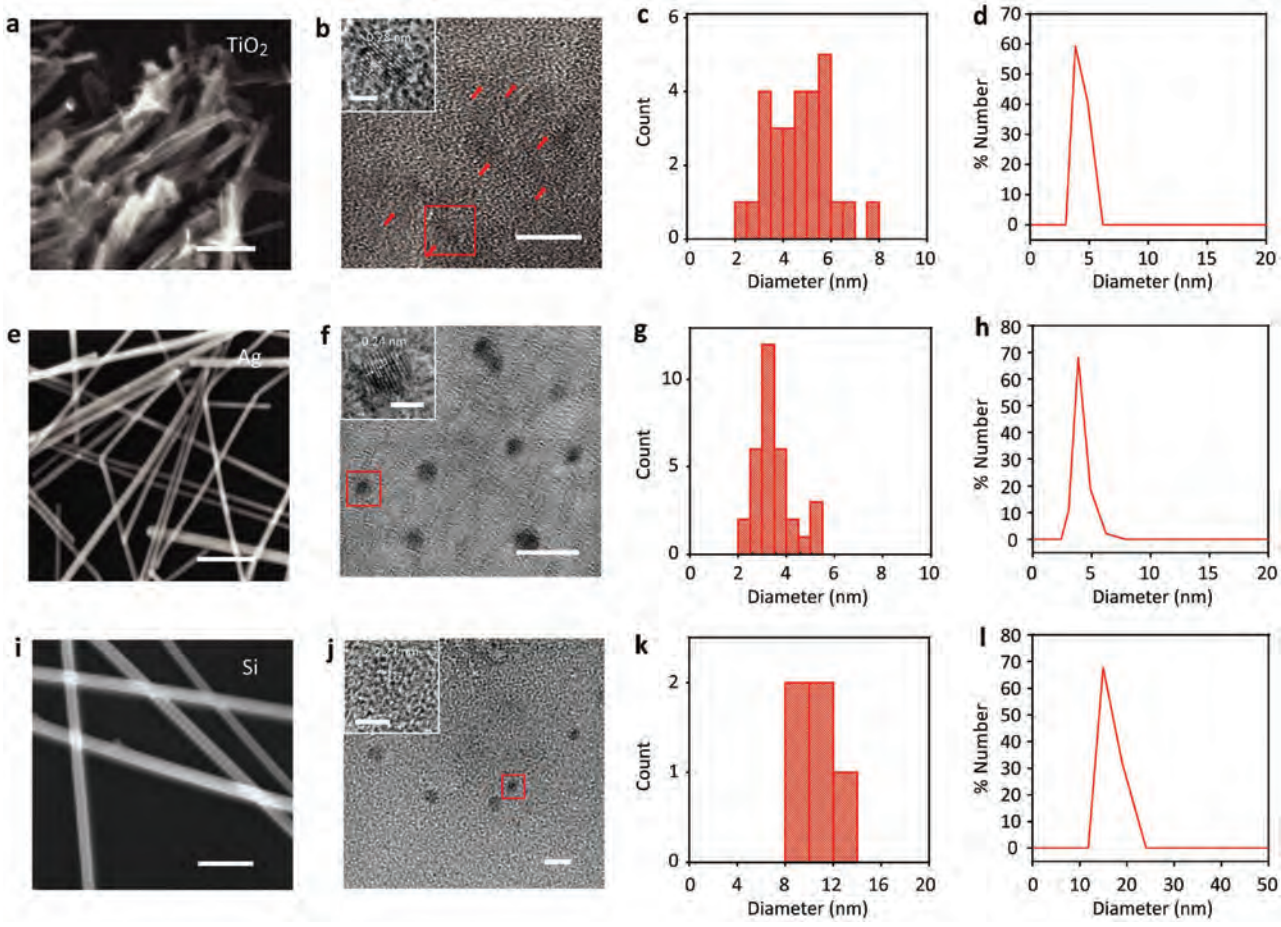

Figure 3. Sonofragmentation of ultrathin oxide, metal, and semiconductor nanowires. a) SEM image of TiO_2 nanowires. Scale bar, 100 nm. b) TEM image of TiO_2 NPs (red arrows) after 24 h ultrasonication of the TiO_2 nanowires in water. Scale bar, 10 nm. Inset, HRTEM image of a single TiO_2 NP (red box). Scale bar, 2 nm. c) Size distribution of the TiO_2 NPs measured with TEM ($\mu = 4.63$ nm, $\sigma = 1.28$ nm, $n = 27$). d) Size distribution of the TiO_2 NPs measured with DLS in water. e) SEM image of Ag nanowires. Scale bar, 200 nm. f) TEM image of Ag NPs after 24 h ultrasonication of the Ag nanowires in water. Scale bar, 10 nm. Inset, HRTEM image of a single Ag NP (red box). Scale bar, 2 nm. g) Size distribution of the Ag NPs measured with TEM ($\mu = 3.46$ nm, $\sigma = 0.75$ nm, $n = 32$). h) Size distribution of the Ag NPs measured with DLS in water. i) SEM image of Si nanowires. Scale bar, 200 nm. j) TEM image of Si NPs after 24 h ultrasonication of the Si nanowires in DMF. Scale bar, 20 nm. Inset, HRTEM image of a single Si NP (red box). Scale bar, 5 nm. k) Size distribution of the Ag NPs measured with TEM ($\mu = 10.8$ nm, $\sigma = 2.2$ nm, $n = 5$). l) Size distribution of the Si NPs measured with DLS in DMF.

Experimental Section

Sonofragmentation: Sonofragmentation of 1D substrates were carried out using a bench-top bath ultrasonicator (40 kHz, max sonication power 110 W, Bransonic Ultrasonic Baths, Thomas Scientific). Starting materials in powder or suspended form (TiO_2 nanowires, Sigma-Aldrich; Ag nanowires, Novarials Corp.; Ge nanopowder, SkySpring Nanomaterials, Inc.) were added directly to an amber glass vial (4 mL, Sigma-Aldrich) with solvents for ultrasonication. Starting materials attached to a wafer substrate were first gently ultrasonicated in the solvents for 2 min and then the supernatant was transferred to another amber glass vial for subsequent ultrasonication. The bath temperature of the ultrasonicator was not actively controlled unless otherwise noted. The temperature typically increased from about 25 to about 60 °C for the 18 h ultrasonication. Active control of temperature was achieved by using a chiller (RC 2 Basic, IKA Works, Inc.) and the internal heating system of the ultrasonicator for the temperature ranges of 10–20 °C, and 60–65 °C, respectively.

TEM and SEM Characterizations: TEM characterization of the NPs was carried out using a JEM-2100 TEM (JEOL). The as-synthesized NPs were (re)suspended in ethanol (for Ge, TiO_2, and Si NPs) or water (for Ag NPs) before being filtered through a 0.2 µm filter to remove large aggregates and debris. The suspension was then drop-casted on a carbon–copper grid (Ted Pella, Inc.) and dried in a vacuum desiccator for 20 min. The imaging was carried out at 200 keV under bright-field illumination. SEM characterization of the nanowires and fragments was carried out using an UltraPlus FE-SEM (Zeiss) with an inlens detector.

DLS Characterization: DLS characterization of the NPs was carried out with a dynamic light scattering instrument (DynaPro NanoStar, Wyatt Technology Corp.). About 100 uL of the sample was transferred to a disposable cuvette (Wyatte Technology Corp.) for the DLS measurement. The final histogram of NP size distribution was generated from 10 measurements for each sample.

PL and UV–Vis Absorption Characterization: PL characterization of the NPs was carried out using a fluorescence spectrometer (Cary Eclipse, Agilent Technologies, Inc.). About 40 ul of the sample was transferred to a quartz cuvette (Sigma-Aldrich) for the fluorescence measurement. UV–vis spectra of the NPs were measured using a bench-top UV–vis spectrometer (NanoDrop 2000, Thermo Fisher Scientific, Inc.).

FTIR Characterization: FTIR characterization of the Ge NPs was carried out using an FTIR spectrometer (SpectrumOne, PerkinElmer). After 18 h of ultrasonication in DMF, the NPs were dried under vacuum and resuspended in chloroform for three times to completely remove the DMF. The NP chloroform suspension was then drop-casted onto the ATR crystal of the FTIR spectrometer and air-dried for 15 min before the measurement. The FTIR measurement was carried out for 3 min and the baseline was automatically corrected.

Nanowire Synthesis: Ge and Si nanowires were synthesized with vapor–liquid–solid growth mechanism using published protocols.[44,50,51] Briefly, Ge nanowires were grown with 2 nm gold nanocatalyst for 150 min using GeH_4 (2 sccm) and H_2 (18 sccm) at total pressure of 400 torr and temperature of 270 °C. Si nanowires were grown for 60 min with 30 nm gold nanocatalyst using SiH_4 (2.5 sccm) and H_2 (60 sccm) at total pressure of 40 torr and temperature of 450 °C.

Supporting Information

Supporting Information is available from the Wiley Online Library or from the author.

Acknowledgements

E.S.B. acknowledges support from the MIT Media Lab, the New York Stem Cell Foundation-Robertson Investigator Award, NIH Director's Pioneer Award 1DP1NS087724, the DOD MURI program, the Open Philanthropy Project, and NSF INSPIRE Award CBET 1344219. The authors thank Prof. C. M. Lieber and Lieber group members for insightful discussion. This work was performed in part at the Harvard University Center for Nanoscale Systems (CNS), a member of the National Nanotechnology Coordinated Infrastructure Network (NNCI), which is supported by the National Science Foundation under NSF award no. 1541959. This work also made use of the MRSEC Shared Experimental Facilities at MIT, supported by the National Science Foundation under award number DMR-1419807. R.G. and I.G. contributed equally to this work.

Received: October 31, 2016
Published online:

[1] B. H. Kim, M. J. Hackett, J. Park, T. Hyeon, *Chem. Mater.* **2014**, *26*, 59.
[2] K. Zarschler, L. Rocks, N. Licciardello, L. Boselli, E. Polo, K. P. Garcia, L. De Cola, H. Stephan, K. A. Dawson, *Nanomedicine* **2016**, *12*, 1663.
[3] K. Ma, U. Werner-Zwanziger, J. Zwanziger, U. Wiesner, *Chem. Mater.* **2013**, *25*, 677.
[4] Z. Li, Q. Sun, Y. Zhu, B. Tan, Z. P. Xu, S. X. Dou, *J. Mater. Chem. B* **2014**, *2*, 2793.
[5] M. Lundqvist, J. Stigler, G. Elia, I. Lynch, T. Cedervall, K. A. Dawson, *Proc. Natl. Acad. Sci. USA* **2008**, *105*, 14265.
[6] A. Albanese, P. S. Tang, W. C. W. Chan, *Annu. Rev. Biomed. Eng.* **2012**, *14*, 1.
[7] Y. Gao, X. Pi, X. Wang, T. Yuan, Q. Jiang, R. Gresback, J. Lu, D. Yang, *Part. Part. Syst. Charact.* **2016**, *33*, 271.
[8] X. Liu, Y. Zhang, T. Yu, X. Qiao, R. Gresback, X. Pi, D. Yang, *Part. Part. Syst. Charact.* **2016**, *33*, 44.
[9] M. Dasog, G. B. los Reyes, L. V Titova, F. A. Hegmann, J. G. C. Veinot, *ACS Nano* **2014**, *8*, 9636.
[10] O. Masala, R. Seshadri, *Annu. Rev. Mater. Res.* **2004**, *34*, 41.
[11] V. Amendola, M. Meneghetti, *Phys. Chem. Chem. Phys.* **2012**, *15*, 3027.
[12] N. Shirahata, D. Hirakawa, Y. Masuda, Y. Sakka, *Langmuir* **2013**, *29*, 7401.
[13] N. Shirahata, M. R. Linford, S. Furumi, L. Pei, Y. Sakka, R. J. Gates, M. C. Asplund, *Chem. Commun.* **2009**, 4684.
[14] T. Prasad Yadav, R. Manohar Yadav, D. Pratap Singh, *Nanosci. Nanotechnol.* **2012**, *2*, 22.
[15] C. Lam, Y. F. Zhang, Y. H. Tang, C. S. Lee, I. Bello, S. T. Lee, *J. Cryst. Growth* **2000**, *220*, 466.
[16] E. Gaffet, *Mater. Sci. Eng. A* **1991**, *136*, 161.
[17] J. A. Luna López, A. Garzón Román, E. Gómez Barojas, J. F. F. Gracia, J. Mart'inez Juárez, J. Carrillo López, *Nanoscale Res. Lett.* **2014**, *9*, 1.
[18] T. Del Cano, L. F. Sanz, P. Martin, M. Avella, J. Jimenez, A. Rodriguez, J. Sangrador, T. Rodriguez, V. Torres-Costa, R. J. Martin-Palma, J. M. Martinez-Duart, *J. Electrochem. Soc.* **2004**, *151*, C326.
[19] G. Kartopu, V. A. Karavanskii, U. Serincan, R. Turan, R. E. Hummel, Y. Ekinci, A. Gunnæs, T. G. Finstad, *Phys. Status Solidi* **2005**, *202*, 1472.
[20] J. Hwang, Y. Jeong, K. H. Lee, Y. Seo, J. Kim, J. W. Hong, E. Kamaloo, T. A. Camesano, J. Choi, *Ind. Eng. Chem. Res.* **2015**, *54*, 5982.
[21] H. Zeng, X. W. Du, S. C. Singh, S. A. Kulinich, S. Yang, J. He, W. Cai, *Adv. Funct. Mater.* **2012**, *22*, 1333.
[22] R. D. Tilley, K. Yamamoto, *Adv. Mater.* **2006**, *18*, 2053.
[23] B. R. Taylor, S. M. Kauzlarich, G. R. Delgado, H. W. H. Lee, L. E. S. Nanocrystals, *Chem. Mater.* **1999**, *11*, 2493.
[24] H. P. Wu, M. Y. Ge, C. W. Yao, Y. W. Wang, Y. W. Zeng, L. N. Wang, G. Q. Zhang, J. Z. Jiang, *Nanotechnology* **2006**, *17*, 5339.
[25] C. R. Stoldt, M. A. Haag, B. A. Larsen, *Appl. Phys. Lett.* **2008**, *93*, 043125.
[26] F. Erogbogbo, T. Liu, N. Ramadurai, P. Tuccarione, L. Lai, M. T. Swihart, P. N. Prasad, *ACS Nano* **2011**, *5*, 7950.
[27] U. Kortshagen, *J. Phys. D: Appl. Phys.* **2009**, *42*, 113001.
[28] H. Ou, Y. Ou, C. Liu, R. W. Berg, K. Rottwitt, *Opt. Mater. Express* **2011**, *1*, 643.
[29] S. Li, I. N. Germanenko, M. S. El-Shall, *J. Cluster Sci.* **1999**, *10*, 533.
[30] K. Das, M. L. N. Goswami, A. Dhar, B. K. Mathur, S. K. Ray, *Nanotechnology* **2007**, *18*, 175301.
[31] S. S. Chang, G. J. Choi, R. E. Hummel, *Mater. Sci. Eng., B* **2000**, *76*, 237.
[32] M. Hoffman, J. G. C. Veinot, *Chem. Mater.* **2012**, *24*, 1283.
[33] S. K. Bux, M. Rodriguez, M. T. Yeung, C. Yang, A. Makhluf, R. G. Blair, J. P. Fleurial, R. B. Kaner, *Chem. Mater.* **2010**, *22*, 2534.
[34] E. J. Henderson, M. Seino, D. P. Puzzo, G. A. Ozin, *ACS Nano* **2010**, *4*, 7683.
[35] A. Gupta, M. T. Swihart, H. Wiggers, *Adv. Funct. Mater.* **2009**, *19*, 696.
[36] Y. Y. Huang, T. P. J. Knowles, E. M. Terentjev, *Adv. Mater.* **2009**, *21*, 3945.
[37] A. Lucas, C. Zakri, M. Maugey, M. Pasquali, P. Van Der Schoot, P. Poulin, *J. Phys. Chem. C* **2009**, *113*, 20599.
[38] J. Stegen, *J. Chem. Phys.* **2014**, *140*.
[39] M. Park, Y. Sohn, W. G. Shin, J. Lee, S. H. Ko, *Ultrason. Sonochem.* **2015**, *22*, 35.
[40] H. B. Chew, M.-W. Moon, K. R. Lee, K.-S. Kim, *Proc. R. Soc. A Math. Phys. Eng. Sci.* **2010**, *467*, 1270.
[41] H.-J. Yang, H.-Y. Tuan, *J. Mater. Chem.* **2012**, *22*, 2215.
[42] S. Kim, B. Walker, S. Y. Park, H. Choi, S.-J. Ko, J. Jeong, M. H. Yun, J. C. Lee, D. S. Kim, J. Y. Kim, *Nanoscale* **2014**, *6*, 10156.
[43] J. Liu, C. Liang, Z. Tian, S. Zhang, G. Shao, *Sci. Rep.* **2013**, *3*, 1741.
[44] L. J. Lauhon, M. S. Gudiksen, C. L. Wang, C. M. Lieber, *Nature* **2002**, *420*, 57.

[45] J. Wang, J. Z. Wang, Z. Q. Sun, X. W. Gao, C. Zhong, S. L. Chou, H. K. Liu, *J. Mater. Chem. A* **2014**, *2*, 4613.
[46] D. Carolan, H. Doyle, *J. Nanomater.* **2015**, *2015*, 1.
[47] A. J. Keung, M. A. Filler, S. F. Bent, *J. Phys. Chem. C* **2007**, *111*, 411.
[48] E. Enache-Pommer, B. Liu, E. S. Aydil, *Phys. Chem. Chem. Phys.* **2009**, *11*, 9648.
[49] H. Mao, J. Feng, X. Ma, C. Wu, X. Zhao, *J. Nanopart. Res.* **2012**, *14*, 887.
[50] Y. Cui, L. J. Lauhon, M. S. Gudiksen, J. Wang, C. M. Lieber, *Appl. Phys. Lett.* **2001**, *78*, 2214.
[51] F. Patolsky, G. Zheng, C. M. Lieber, *Nat. Protoc.* **2006**, *1*, 1711.
[52] Y. Wu, Y. Cui, L. Huynh, C. J. Barrelet, D. C. Bell, C. M. Lieber, *Nano Lett.* **2004**, *4*, 433.
[53] S. Pradhan, S. Chen, J. Zou, S. M. Kauzlarich, *J. Phys. Chem. C* **2008**, *112*, 13292.
[54] S. Yang, W. Li, B. Cao, H. Zeng, W. Cai, *J. Phys. Chem. C* **2011**, *115*, 21056.
[55] B. W. Zeiger, K. S. Suslick, *J. Am. Chem. Soc.* **2011**, *133*, 14530.
[56] J. R. G. Sander, B. W. Zeiger, K. S. Suslick, *Ultrason. Sonochem.* **2014**, *21*, 1908.
[57] T. Saito, R. Kuramae, J. Wohlert, L. A. Berglund, A. Isogai, *Biomacromolecules* **2013**, *14*, 248.
[58] W. B. McNamara, Y. T. Didenko, K. S. Suslick, *Nature* **1999**, *401*, 772.
[59] H. Y. Peng, Z. W. Pan, L. Xu, X. H. Fan, N. Wang, C. S. Lee, S. T. Lee, *Adv. Mater.* **2001**, *13*, 317.
[60] R. W. Day, M. N. Mankin, R. Gao, Y.-S. No, S.-K. Kim, D. C. Bell, H.-G. Park, C. M. Lieber, *Nat. Nanotechnol.* **2015**, *10*, 345.
[61] M. Y. Tsai, C. Y. Yu, C. C. Wang, T. P. Perng, *Cryst. Growth Des.* **2008**, *8*, 2264.
[62] T. Hanrath, B. A. Korgel, *J. Am. Chem. Soc.* **2004**, *126*, 15466.

Particle
& Particle Systems Characterization

Supporting Information

for *Part. Part. Syst. Charact.,* DOI: 10.1002/ppsc.201600339

Sonofragmentation of Ultrathin 1D Nanomaterials

*Ruixuan Gao, Ishan Gupta, and Edward S. Boyden**

Supporting Information

Sonofragmentation of ultra-thin 1D nanomaterials

*Ruixuan Gao, Ishan Gupta, and Edward S. Boyden**

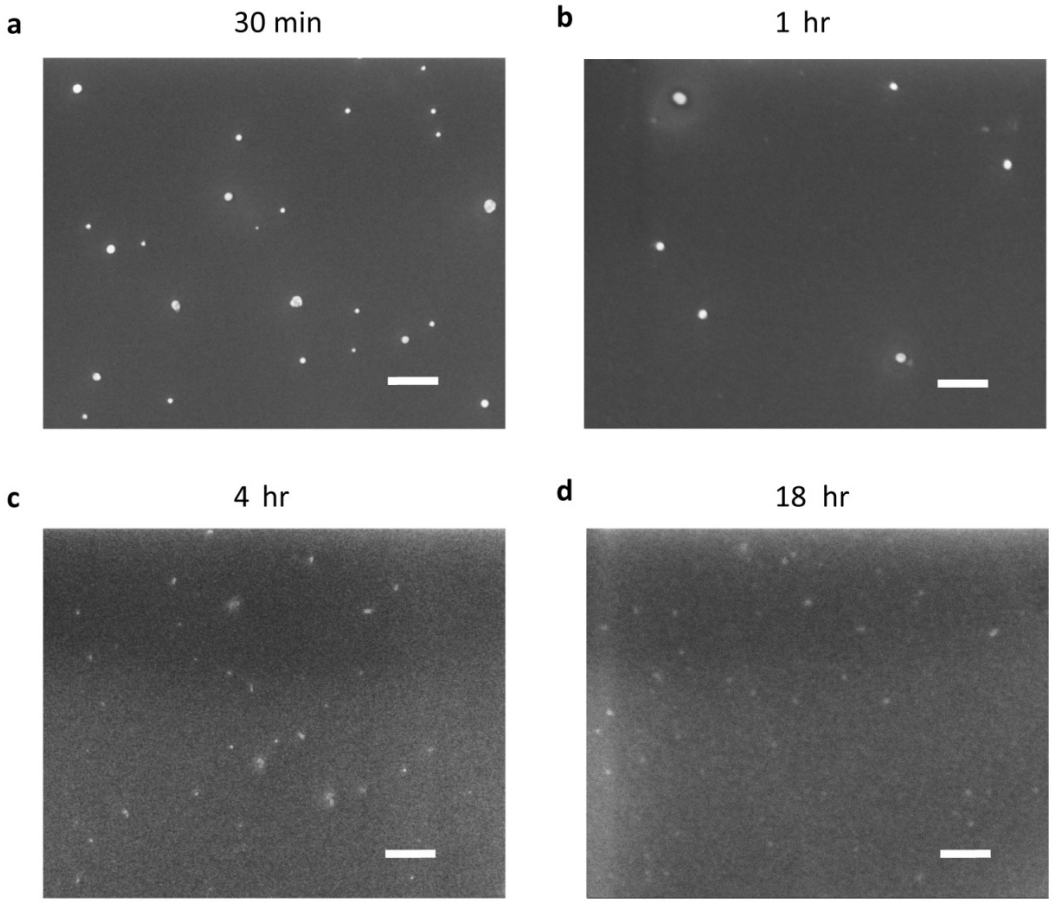

Figure S1. Scanning electron microscope (SEM) images of ultrasonicated Ge nanowires in DMF after a) 30 min, b) 1 hr, c) 4 hrs and d) 18 hrs of continuous ultrasonication. The samples were resuspended in ethanol before drop-casted to a Si substrate for the SEM imaging. Scale bars, 200 nm.

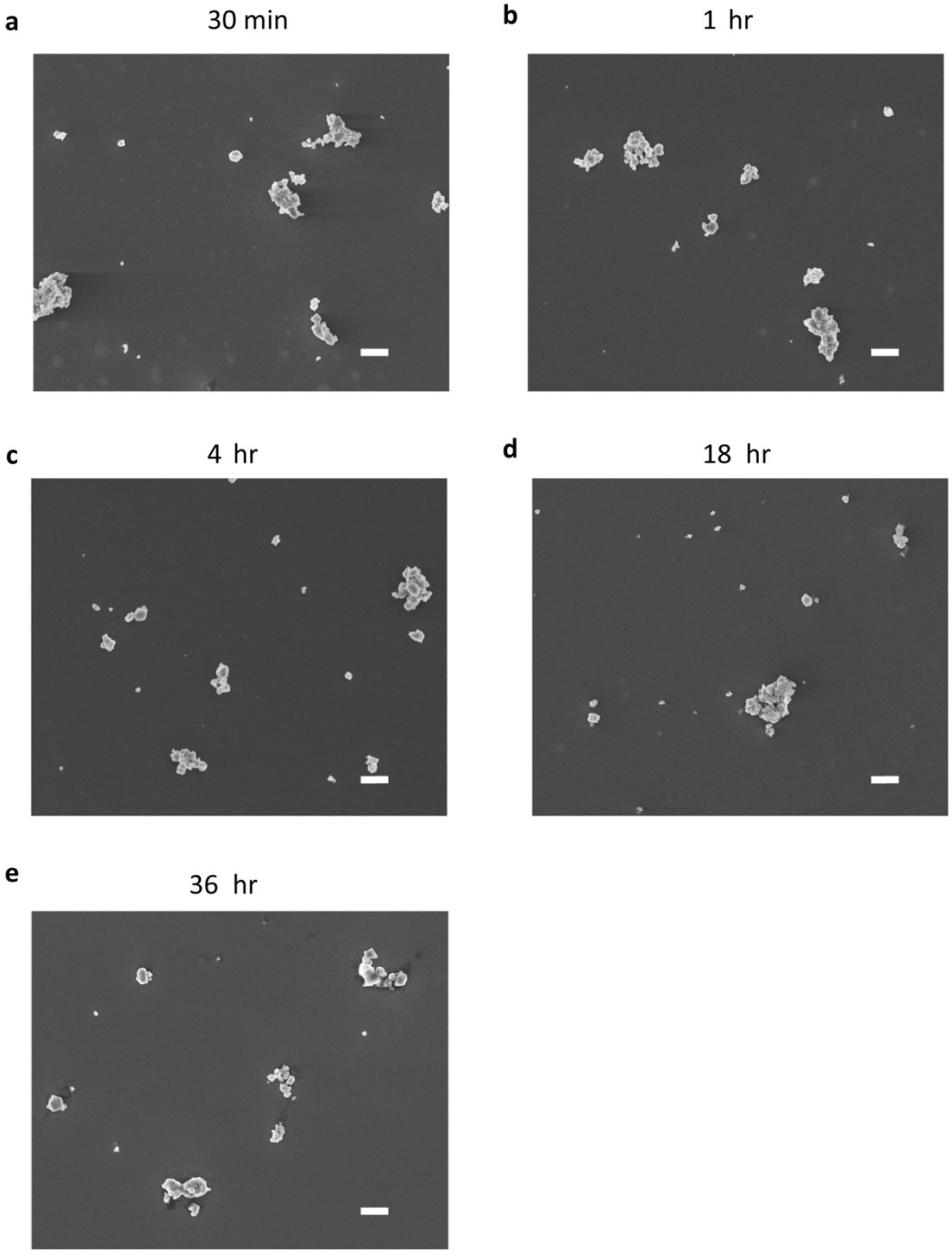

Figure S2. SEM images of ultrasonicated Ge nanopowder (~100-300 nm dimeter) in DMF after a) 30 min, b) 1 hr, c) 4 hrs, d) 18 hrs and e) 36 hrs of continuous ultrasonication. The samples were resuspended in ethanol before drop-casted to a Si substrate for the SEM imaging. Scale bars, 1 μm.

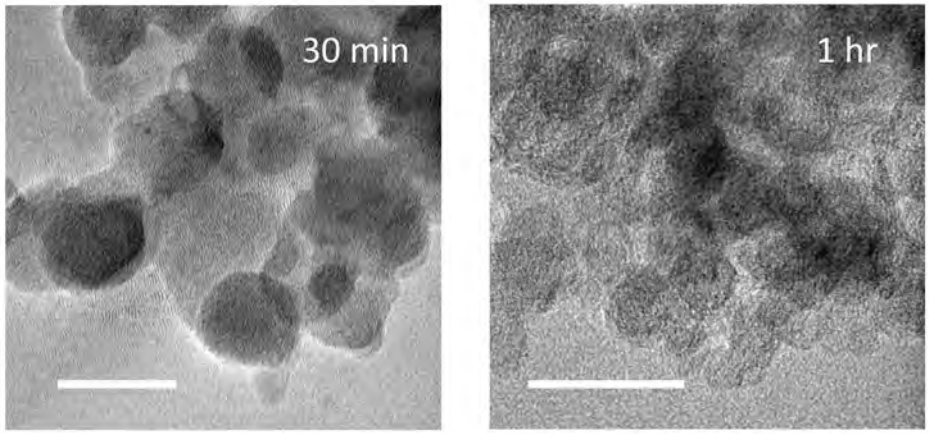

Figure S3. Transmission electron microscope (TEM) images of sonofragmented Ge nanoparticles (Ge NPs) after 30 min (left) and 1 hr (right) of continuous ultrasonication of Ge nanowires in DMF. The samples were resuspended in ethanol before drop-casted to a carbon-copper grid and dried in a vacuum desiccator for 20 min. Scale bars: 50 nm.

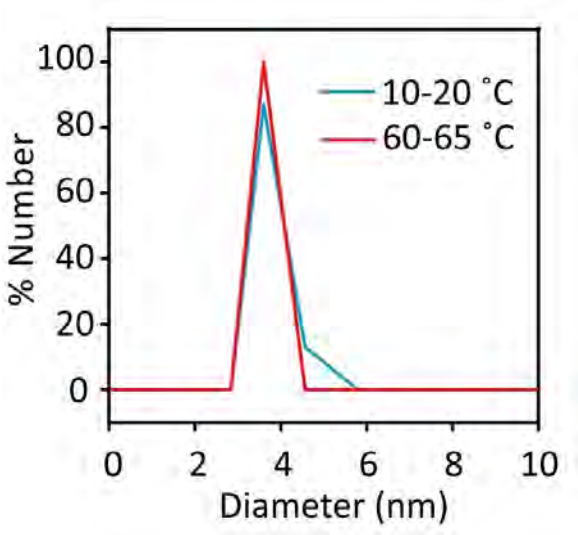

Figure S4. Size distribution of Ge NPs after 18 hr ultrasonication of Ge nanowires in DMF at 10-20 °C (blue) and 60-65 °C (red). The nanoparticle size was measured with dynamic laser scattering (DLS) in DMF.

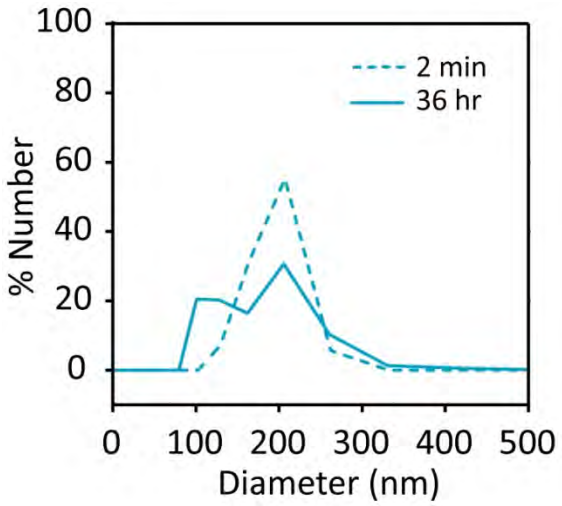

Figure S5. Size distribution of Ge NPs measured with DLS after 2 min (dotted blue) and 36 hrs (solid blue) of ultrasonication of Ge nanopowder in DMF.

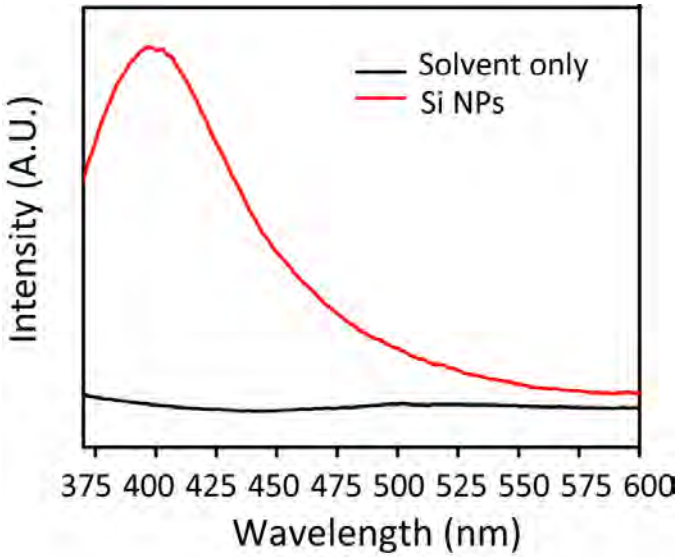

Figure S6. Photoluminescence **(**PL) of Si NPs in ethanol under 320 nm UV-illumination. Ultrasonication was carried out in DMF for 24 hrs and the solvent was exchanged to ethanol for the PL measurement.